Crystal Structure of Interleukin 10 Reveals an Interferon γ-like Fold[†,‡]

Mark R. Walter*[,§] and T. L. Nagabhushan[||]

Department of Pharmacology and Center for Macromolecular Crystallography, University of Alabama at Birmingham, Birmingham, Alabama 35294, and Schering Plough Research Institute, Kenilworth, New Jersey 07033

Received May 26, 1995; Revised Manuscript Received July 12, 1995[⊗]

ABSTRACT: The crystal structure of recombinant human interleukin 10 (rhIL-10) has been determined by X-ray crystallography at 2.0 Å resolution. Interleukin 10 is a dimer composed of identical polypeptide chains related by a 2-fold axis. The molecule is predominantly α-helical. The main-chain fold resembles that of interferon γ (IFN-γ) in which the structural integrity of each domain is dependent on the intertwining of helices from each peptide chain. Comparison of rhIL-10 and IFN-γ reveals differences in helix lengths and orientations of the 2-fold related domains. Interleukin 10 and IFN-γ contain several conserved residues in their internal cores which suggest a possible "fingerprint" for detection of other members of this fold.

Interleukin 10 (IL-10) is a product of T_H2 helper T-cells (Fiorentino et al., 1989), B cells (Suda et al., 1990), monocytes, and macrophages (de Waal Malefyt et al., 1991a). Originally named cytokine synthesis inhibitory factor, IL-10 was first identified by its ability to inhibit the synthesis of cytokines from activated T_H1 helper T-cells including interferon γ (IFN-γ),[1] interleukin 2, interleukin 3, tumor necrosis factor β, and granulocyte macrophage colony stimulating factor (de Waal Malefyt et al., 1991a). Further studies have elucidated numerous immunosuppressive and immunostimulatory activities for IL-10 on a broad range of cell types. Specifically, IL-10 downregulates the expression of major histocompatability complex (MHC) class II antigens on monocytes and suppresses the release of reactive oxygen intermediates (de Waal Malefyt et al., 1991b; Fiorentino et al., 1991; Bogdan et al., 1991). It enhances the viability, proliferation, and upregulation of class II MHC expression in murine B-cells (Go et al., 1990; Defrance et al., 1992; Rousset et al., 1992). In addition, IL-10 costimulates the growth of stem cells (Rennick et al., 1992), thymocytes (MacNeil et al., 1990), and mast cells (Thompson-Snipes et al., 1991; Rennick et al., 1994) and enhances the generation of cytotoxic T-cell activity (Chen et al., 1991).

Interleukin 10's pleotropic activities are conveyed to cells by a high-affinity ($K_d = 10^{-10}$ M) interaction with its cell surface receptor (IL-10R). The IL-10R is a member of the class 2 cytokine receptor family (Bazan, 1990; Ho et al., 1993; Liu et al., 1994) which also includes the cellular receptors for interferon α, β (Uze et al., 1990; Novick et al., 1994) and γ subtypes (Aguet et al., 1988) and the membrane tether for coagulation protease factor VII, tissue factor. The extracellular portions of the receptors share a modular architecture consisting of a tandem set of fibronectin domains that are distinguished by unique cysteine sequence patterns (Bazan, 1990). Cell signaling is believed to occur by ligand-induced receptor oligomerization (Heldin, 1995).

Isolation and expression of the cDNA clones for human (hIL-10) and murine IL-10 (mIL-10) reveal mature proteins of 160 and 157 amino acids, respectively (Moore et al., 1990; Vieira et al., 1991). The proteins, which exist in solution as noncovalent homodimers (Tan et al., 1993), exhibit an overall sequence identity of 74%. Additional nucleotide sequence comparisons have identified IL-10 homologs in the Epstein Barr virus (BCRF1) and equine herpes virus type II (Moore et al., 1990; Vieira et al., 1991; Rode et al., 1993). Biological assays with BCRF1 show that it exhibits some but not all of the activities of human or murine IL-10 (Hsu et al., 1990).

Initial biophysical characterization of human and murine IL-10 has established the presence of two disulfide bonds which link the first and third and the second and fourth cysteine residues (Windsor et al., 1993). Furthermore, CD analysis indicates that each protein is predominantly α-helical. On the basis of these initial characterizations and sequence analysis, IL-10 was predicted to adopt a long-chain cytokine fold (Sprang & Bazan, 1993) which is exhibited by the crystal structures of growth hormone (GH) (Abdel-Meguid et al., 1987; de Vos et al., 1992; Ultsch et al., 1994), granulocyte colony stimulating factor (G-CSF) (Hill et al., 1993; Lovejoy et al., 1993), interferon β (IFN-β) (Senda et al., 1992), and leukemia inhibitory factor (LIF) (Robinson et al., 1994).

While extensive data exist on the biological properties of IL-10, the structural basis of the ligand−receptor interaction is largely uncharacterized. Here we report the 2.0 Å crystal structure of recombinant human IL-10 (rhIL-10). Unexpectedly, rhIL-10 exists as an intercalated dimer as first observed for IFN-γ (Ealick et al., 1991; Samudzi et al., 1991). Comparison of IL-10 and IFN-γ reveals a conserved five-residue core which is conserved in all species of both cytokines. On the basis of the structural identity with IFN-γ, a potential site of interaction with its receptor is presented.

[†] This work was supported by grants to M.R.W. from the Pharmaceutical Manufacturers Association and NCI Grant CA13148, Junior Faculty Development Award.

[‡] Coordinates have been deposited with the Brookhaven Protein Data Bank under the file name 1INR.

* Send correspondence to this author at the Department of Pharmacology [email, walter@mimas.cmc.uab.edu].

[§] University of Alabama at Birmingham.

[||] Schering Plough Research Institute.

[⊗] Abstract published in *Advance ACS Abstracts,* September 15, 1995.

[1] Abbreviations: rhIL-10, recombinant human interleukin 10; IL-10R, interleukin 10 receptor; IFN-β, interferon β; IFN-γ, interferon γ; GH, growth hormone; G-CSF, granulocyte colony stimulating factor; LIF, leukemia inhibitory factor; F_o, observed structure factor; F_c, calculated structure factor.

0006-2960/95/0434-12118$09.00/0

Table 1: Heavy-Atom and Data Collection Statistics

data set	R_{merge}[a] (%)	measurements (no. of crystals)	unique	resolution (Å)	coverage (%)	MFID[b]	no. of sites	R_{cen}[c]	phasing power[d]
native (R-AXIS)	6.27	40 447 (2)	5 025	2.5	85				
10 mM $K_3UO_2F_5$	4.13	25 677 (1)	3 884	2.8	96	8.4	4	56.7	1.44
20 mM $K_3UO_2F_5$	5.80	21 116 (1)	3 917	2.8	99	11.8	3	58.3	1.38
native (EMBL)	8.04	42 251 (3)	10 087	2.0	92				

[a] $R_{merge} = \sum|I_h - \langle I_h\rangle|/\sum I_h$, where $\langle I_h\rangle$ is the average over multiple observations. [b] MFID = mean fractional isomorphous difference, $\sum|F_{PH} - F_P|/\sum F_{PH}$, where F_{PH} and F_P are the derivative and native structure factor amplitudes, respectively. [c] $R_{cen} = \sum||F_{PH(obs)}| \pm F_{P(obs)}| - F_{H(calc)}|/\sum|F_{PH(obs)} - F_{P(obs)}|$ for centric reflections. [d] Phasing power = $|F_{H(calc)}|/|F_{PH(obs)} - F_{PH(calc)}|$.

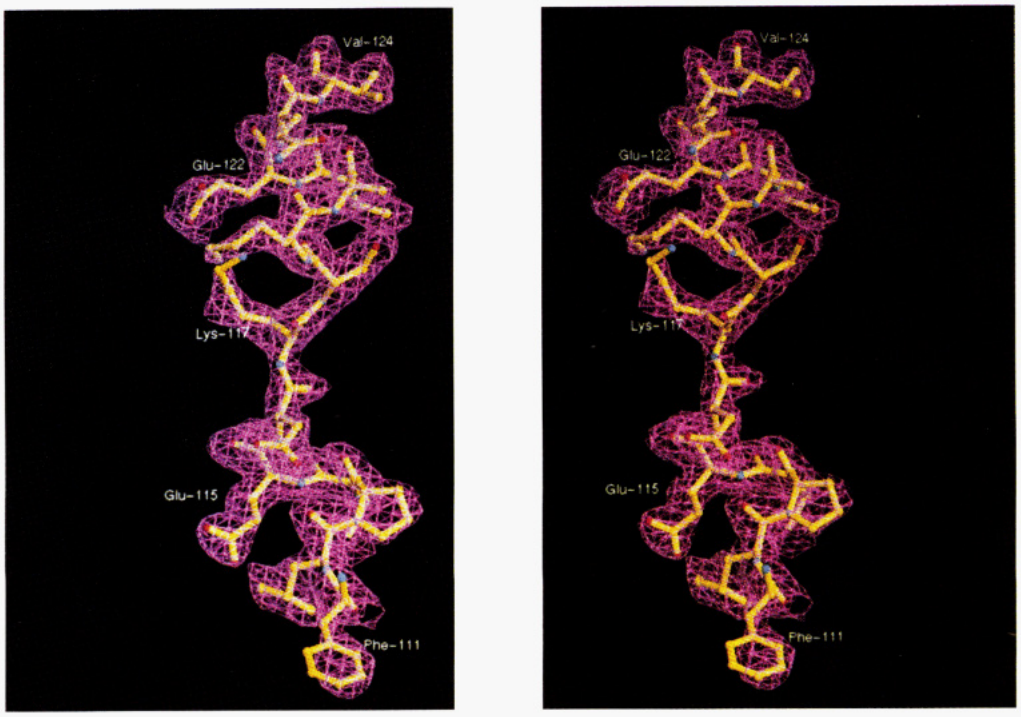

FIGURE 1: Stereoview of electron density ($2F_o - F_c$ at $1\sigma,\alpha_{calc}$ phases) and refined model of rhIL-10 for residues 111−124 in the domain crossover. Selected residues are labeled. All figures, except Figures 2 and 5, were made with the program Ribbons (Carson, 1991).

MATERIALS AND METHODS

Crystals of recombinant human IL-10 were grown from ammonium sulfate solutions using macroseeding as previously described (Cook et al., 1995). Briefly, crystalline aggregates of IL-10 were grown from 35% ammonium sulfate in 100 mM HEPES buffer at pH 7.2. Small perfect crystals for macroseeding were obtained by streaking new drops with a needle used to crush the initial aggregates. Crystals for data collection were grown by transferring the seed crystals into 2 μL drops containing 20 mg/mL IL-10 and 40% ammonium sulfate in 100 mM HEPES buffer, pH 7.2. The drops were equilibrated against a 1 mL well of 40% ammonium sulfate solution described above. Tetragonal bipyramid-shaped crystals (0.20 × 0.20 × 0.60 mm^3) of rhIL10 belong to the space group $P4_32_12$ with unit cell dimensions of $a = 36.56$ Å and $c = 220.97$ Å. There is the equivalent of one molecule in the crystallographic asymmetric unit, and the solvent volume fraction is approximately 38%. Potential heavy-atom derivatives were prepared by soaking crystals of rhIL-10 for 24 h at 22 °C in 60% saturated ammonium sulfate solutions that contained 100 mM HEPES buffer at pH 7.2.

For heavy-atom screening, intensity data were collected with an R-AXIS IIc image plate detector using Cu Kα radiation from a Rigaku RU-200 rotating anode generator. The data were integrated and scaled using the software provided by Molecular Structure Corp. Most data manipulations were carried out using the CCP4 suite of programs (CCP4, 1994). While two derivatives were quickly identified ($KAuCl_4$ and K_2PtCl_4) by interpretation of difference Patterson maps, their phasing power was limited to about 6 Å resolution. Subsequently, two highly isomorphous derivatives (10 mM and 20 mM $K_3UO_2F_5$) were identified by inspection of difference Fourier maps calculated with phases obtained with the $KAuCl_4$ and K_2PtCl_4 compounds (Table 1).

A 2.8 Å phase set was generated using the two $K_3UO_2F_5$ derivatives (10 and 20mM) including the anomalous data. The figure of merit (FOM) for 3784 reflections was 0.50. The phases were modified by solvent leveling and histogram matching as implemented in the program DM (Cowtan, 1994). The DM modified phases (FOM =0.75) produced an interpretable electron density map for residues 23−35, 46−107, and 111−156. The full atom model of rhIL10 was built using the graphics program CHAIN (Sack, 1988). Confidence in the chain tracing of rhIL10 was gained due to strong electron density for the disulfide bond between Cys-62 and Cys-114, the connection between helices D and E (Figure 1), and the overall agreement of the sidechain density for each amino acid residue. In addition, the observed heavy-atom positions made chemical sense with the location of sidechain groups in the structure.

Table 2: Refinement Statistics

no. of protein atoms	1075
no. of solvent atoms	42
resolution range (Å)	10.0−2.0 Å
unique data used	9988
R-factor (%)	22.1
free *R*-factor (%)	33.7
rms deviations	
bond distance (Å)	0.02
bond angle (deg)	3.79
dihedral angles (deg)	21.84
improper angles (deg)	1.57
B-factors, bonded (Å^2)	3.75

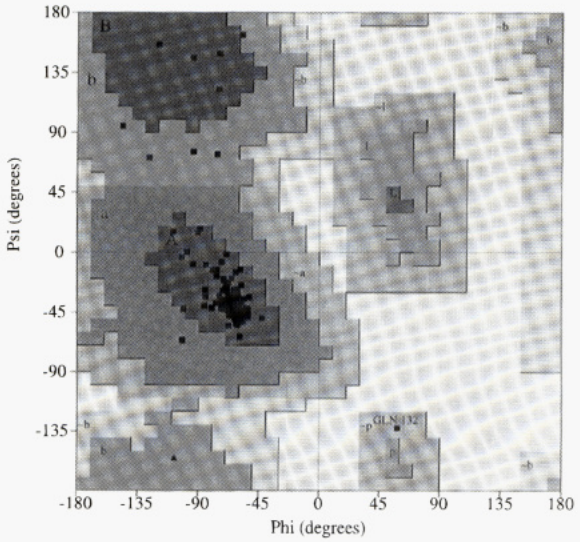

FIGURE 2: Ramachandran plot for the final model of rhIL-10. Glycines are denoted as triangles and all others as squares. The calculation and figure were obtained using the program Procheck (Morris et al., 1992).

Recombinant human IL-10 was refined by simulated annealing using the program X-PLOR (Brunger, 1992a) against a 2 Å resolution data set collected at the EMBL outstation (DESY, Station BW7B, Table 1). The data were integrated and scaled using the programs DENZO and SCALEPACK (Otwinowski, 1993). A randomly selected 10% of the data were removed prior to refinement for analysis of the free *R*-factor (Brunger, 1992b). Alternate cycles of X-PLOR refinement and manual model building using $2F_o - F_c$ and $F_o - F_c$ maps with calculated 2 Å phases yielded the final model of IL-10 which contains residues 18−37, 45−107, and 111−159 and 42 water molecules. The force-field parameters from the molecular dynamics program CHARMM (Brooks et al., 1989) were used for refinement with the modifications described by Brunger et al. (1989). The *R*-factor based on all 9888 reflections between 10 and 2.0 Å is 22.1% ($R = 20.9\%$ for data greater that 3σ) with an R_{free} of 33.7% for 1117 atoms. The data are 71% complete (working set) in the 2.1−2.0 Å shell. The root-mean-square deviations from ideality are 0.02 Å for bond distances and 3.79° for angles (Table 2). All residues fall within allowable regions of ϕ,ψ space with more than 90% of the residues in the most favored region of the Ramachandran plot (Figure 2). The average *B*-factor for the structure is 31.7 Å^2. Comparison of rhIL-10 with other cytokines was done as follows: Cytokine superpositions were first aligned visually on the computer graphics and optimized using the algorithm of Kabsch (1976). Residues in the structural alignments are defined as equivalent if they are within 2.5 Å of one another.

FIGURE 3: Ribbon diagram of the rhIL-10 dimer. The peptide chains are colored orange and blue, respectively. The six α-helices of each chain are labeled consecutively A−F and A′−F′. For completeness, unobserved residues in the AB and DE loops are shown in yellow. The disulfide bond (Cys-62−Cys-114) is represented by white cylinders while the Sγ atoms are shown as gold spheres.

RESULTS

Recombinant human interleukin 10 is a dimer with overall dimensions of 30 × 40 × 70 Å^3. Each monomer consists of six α-helices (labeled A−F) which tightly associate with the 2-fold related molecule (labeled A′-F′) to form an intertwined dimer (Figure 3). The dimer contains two distinct structural domains which are oriented at right angles to one another. Each of the domains are composed of helices A, B, C, and D from one chain and helices E′ and F′ from the other (Figure 4). Although secondary structural elements are shared from each peptide chain as observed for IFN-γ (Ealick et al., 1991; Samudzi et al., 1991) and IL-5 (Milburn et al., 1993), each domain forms a four-helix bundle motif (helices A, C, D, F′ and helices A′, C′, D′, F) similar to the long-chain monomeric cytokines which include IFN-β, G-CSF, GH, and LIF. The helices are connected by three tight turns (BC, CD, and EF loops) and two extended loops (AB and DE loops) on either end of the bundle.

Consistent with CD measurements, the six α-helices of rhIL-10 comprise about 67% of the structure (Windsor et al., 1993). The helices range in length from 7 to 23 residues (Figure 5). All six helices contribute residues to the internal hydrophobic core of the molecule which consists predominantly of leucine and phenylalanine residues. To optimize the packing of the core, helices A, C, and F contain significant bends. The α-helical hydrogen-bonding pattern of helix A is disrupted by two kinks centered at Leu-23 and Phe-30. For the first kink, substitute hydrogen bonds are formed by three ordered water molecules. The waters form a hydrogen bond network between the carbonyl oxygens of Pro-21 and Met-22 of helix A, with the carbonyl oxygen of Asn-97 and Nε1 of Arg-104 from helix D. The side-chain Oγ of Ser-31 and the Nε1 of Arg-32 form a bifurcated hydrogen bond to the carbonyl oxygen of Asp-28 to satisfy the hydrogen bonding for the second kink. Residues following the second kink (residues 33−37) form a short segment of 3_{10} helix. Due to the presence of Pro-78, which is conserved for all known IL-10 amino acid sequences, helix C contains a bend of approximately 23° centered at Val-76.

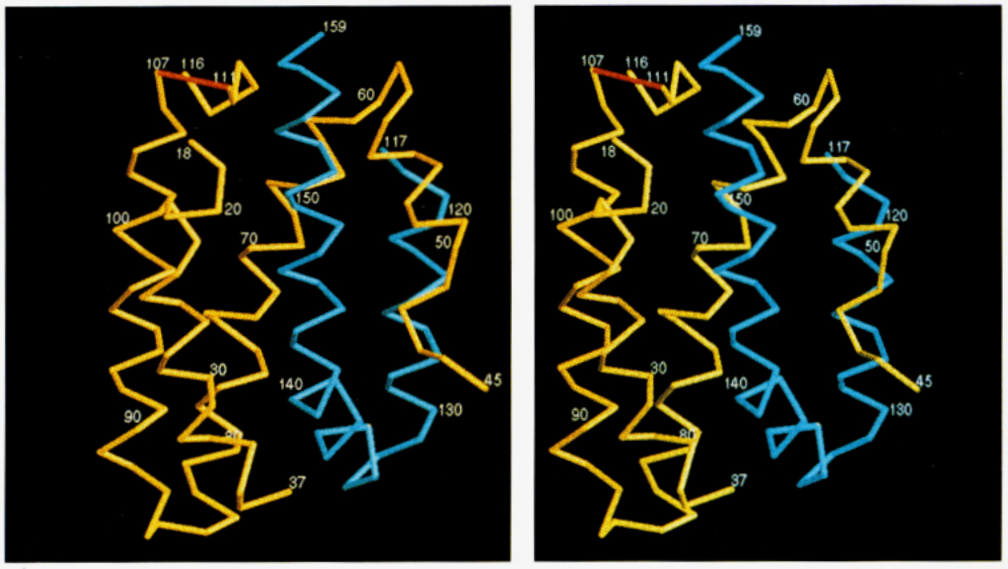

FIGURE 4: Stereoview of the Cα carbon tracing of the rhIL-10 domain. Residues 18−116 from one peptide chain are colored yellow, and residues 117−159 from the 2-fold related chain are colored cyan. Every tenth residue is labeled. The disordered DE loop (residues 108−110) is represented by a red line.

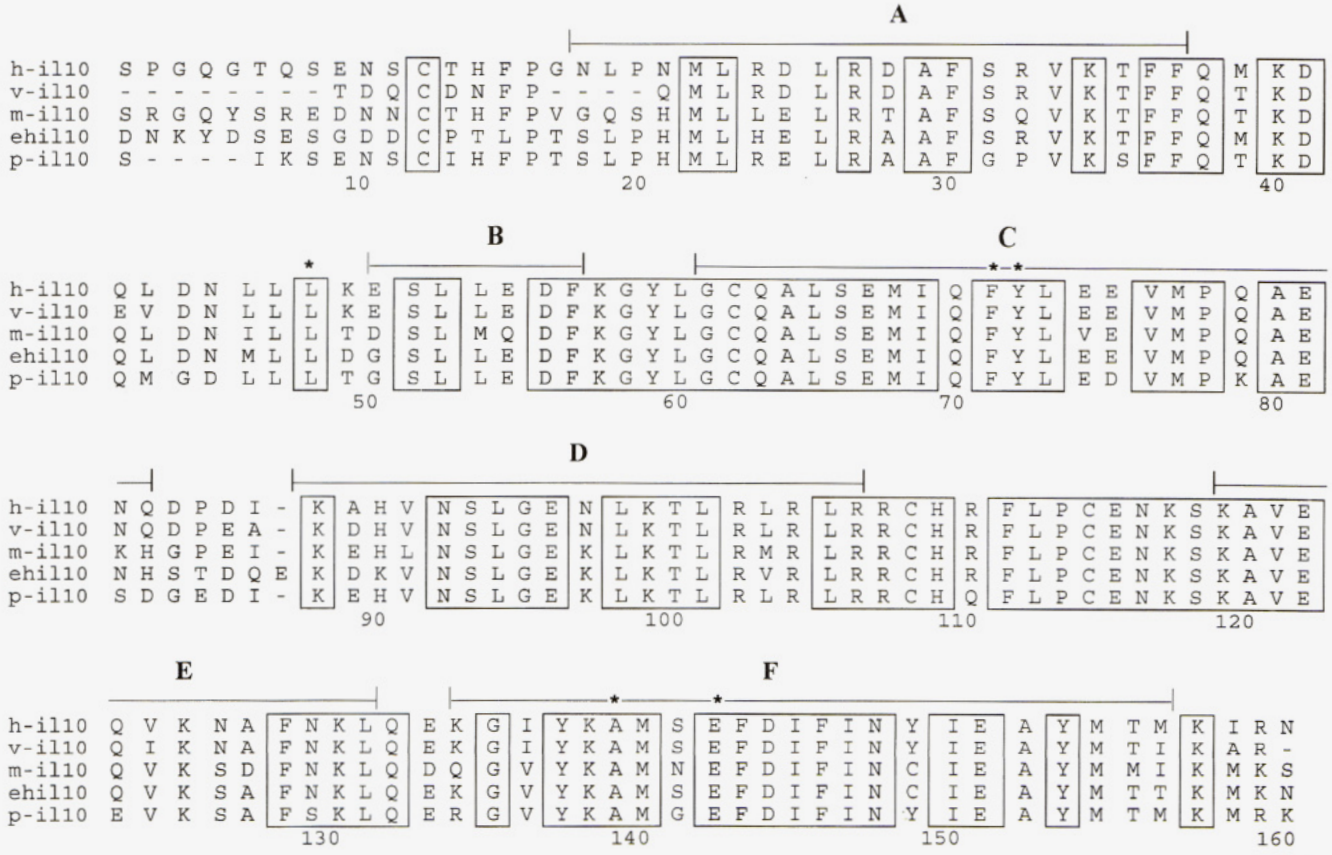

FIGURE 5: Amino acid sequences of IL-10 derived from human (h-IL10; Vieira et al., 1990), Epstein Barr virus (BCRF1 or v-il10), murine (m-IL10; Moore et al., 1990), equine herpes virus type II (ehIL10; Rode et al., 1993), and porcine (p-IL10; Blancho et al., 1995) cDNA sequences. The secondary structural assignments based on crystal structure are noted above the residues. Conserved amino acid residues in all IL-10 sequences available in the SWISS PROT database including rat and bovine (Goodman et al., 1992; Feng et al., 1993; Hash et al., 1994) are boxed. Residues that are conserved in all sequences of IL-10 and IFN-γ are highlighted with asterisks.

Prior to the bend, the helix has unwound such that residues 71−77 form a five-turn helix as described by Kabsch and Sander (1983). The main-chain conformation of the eight residues of the helix is identical to the helix observed for residues 181−188 of alcohol dehydrogenase (Protein Data Bank code 4ADH). The result of the π helix is to form a bulge in helix C at Glu-75. It is unknown if the bulge plays a direct role in orienting Glu-75 for interaction with its receptor or is an evolutionary trick that allows IL-10 to accommodate an extra residue in helix C. Helix F exhibits a pronounced bend of about 129° centered on Glu-142. The bend in the helix exposes the carbonyl oxygen of Ala-139 to the interior of the molecule. A substitute hydrogen bond for the carbonyl oxygen of Ala-139 is formed with the OH of Tyr-72 located on helix C. Tyrosine-72, Ala-139, and Glu-142 are conserved in all 12 amino acid sequences of IL-10, suggesting that the bend in helix F is found in all species of IL-10.

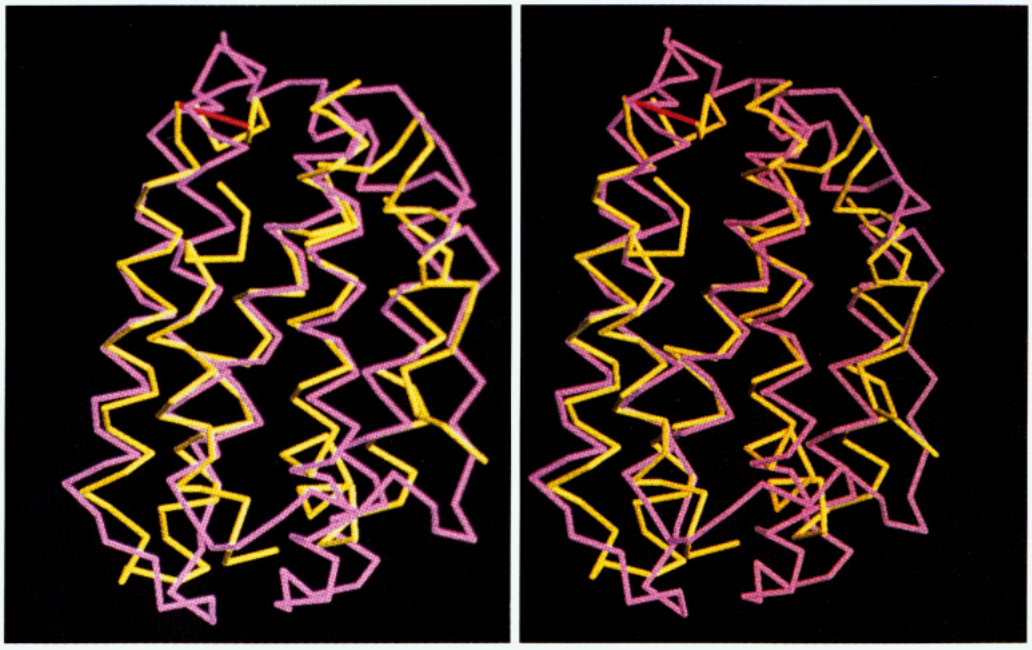

FIGURE 6: Stereoview of the superposition of the rhIL-10 (yellow) and IFN-β (magenta) domains. The view is identical to that in Figure 4.

In contrast to the tightly packed core, the main-chain residues 1−17, 38−44, 108−110, and 160 are disordered in the structure. These flexible regions, which are solvent exposed, cluster on opposite ends of the helical bundle in the N- and C-termini and the extended AB and DE loops. Included in the disordered regions are Cys-12 and Cys-108 which form one of two disulfide bonds in rhIL-10 (Windsor et al., 1993). Cysteine-12 is part of 17 residues at the N-terminus for which no interpretable density was observed. Cysteine-108 is part of a much smaller segment of three disordered residues on the DE loop. Although the disulfide bond and surrounding residues may be modeled, the lack of clear electron density for the bond suggests it is not formed in the crystal. The amount of disorder in the loops caused by the absence of the disulfide bond is unclear. In contrast to the first disulfide linkage, well-ordered electron density is observed for the second between Cys-62 and Cys-114 which fastens the DE loop to the N-terminal end of helix C. Our structural results are consistent with the extreme sensitivity of rhIL-10 to reducing agents, although none were present in the protein preparations or crystallization experiments. Other disordered regions in the structure are residues 38−44 which are located in the center of the AB loop which encircles helix F′ and the C-terminal asparagine residue.

As predicted, the domain architecture of rhIL10 is analogous to the structures of GH, IFN-β, G-CSF, and LIF which are classified as long-chain cytokines (Sprang & Bazan, 1993). Each domain of rhIL-10 shares all common structural features with the other long-chain cytokines including longer helices (~20 amino acids) and the distinct packing of the AB loop over helix F′ and the E′F′ loop (the E′F′ loop of rhIL-10 corresponds to the CD loop in GH, G-CSF, and LIF). Of these four structures, the greatest structural identity with rhIL-10 occurs with G-CSF (Cα pairs 67, rms deviation 1.53 Å) and IFN-β (Cα pairs 64, rms deviation 1.57 Å). All of the equivalencies between rhIL-10 and G-CSF are located in helices A, C, D, and F′, which reflect the structural similarity of their four helix bundles. In contrast, an extremely poor structural correlation is observed for the AB and E′F′ (CD loop in G-CSF) loops. The path of the AB loop of G-CSF overlays onto helix E′ of rhIL-10 rather than helix B, while the CD loop has no equivalent in rhIL-10. For IFN-β, equivalent residues are located on helices A, C, D, E′, and F′ (Figure 6). In addition, the path of the AB loop in IFN-β, which exists in an extended conformation, corresponds to helix B in rhIL-10. While IFN-β displays the best overall structural identity with the domains of rhIL-10, the cytokines do not share any significant sequence homology.

While each domain of rhIL-10 resembles the long-chain monomeric cytokines, the dimer fold of the rhIL-10 is most like the structure of interferon γ (Figure 7). The two most notable differences in the dimers are the size and orientation of the domains. In rhIL-10, the helix bundles are perpendicular to one another, while in IFN-γ the domains are oriented at an angle of about 60°. The domains of rhIL-10 are constrained to exhibit the 90° interdomain angle due to the conformations of the crossover connections which are formed from residues 115 to 118 and 115′ to 118′ (Figure 1). Residues on each end of the crossover connection form interactions with the domains which stabilize and orient the connections and subsequently the domains at 90° to one another. Specific interactions are the symmetry-related Cys-62−Cys-114 disulfide bond and the β-turn composed of residues 113−116 on the N-terminal end of the crossover and the interaction of the Oγ of Ser-118 with Oδ2 of Asp-55 on the C-terminal end of the crossover. Additional interactions between the domains in rhIL-10 occur between the 2-fold related peptide segments (59−63 and 112−116) which form the BC, B′C′ and DE, D′E′ loops. As a result of the 90° interdomain angle, none of the helices of either domain are occluded from potential interactions with the IL-10 receptor. In contrast, the IFN-γ interactions at the dimer interface are made up predominantly from the hydrophobic C-helix. Thus, most of helix C is buried in the dimer interface and not accessible for potential interactions with its cell surface receptors. The differences in the domain orientations are best described by accessible surface calculations. The accessible surface area buried upon dimerization (chain 1 + chain 2) is approximately 8742 Å^2 for IL-10 and

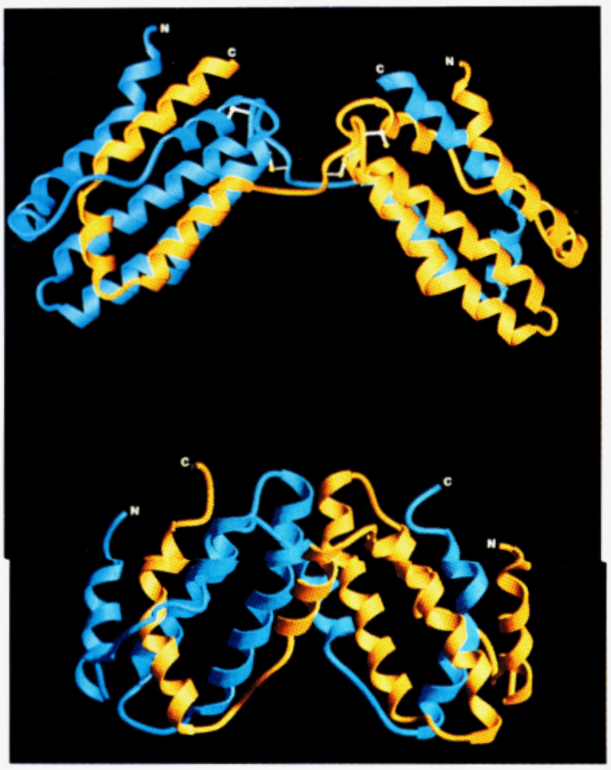

FIGURE 7: Comparison of the domain topology and interdomain angles of rhIL-10 (top of figure) and human IFN-γ (bottom of figure). Each peptide chain of rhIL-10 and IFN-γ is colored yellow and blue, respectively. For completeness, the disordered AB and DE loops of rhIL-10 have been modeled.

7600 Å^2 for IFN-γ. In contrast, the surface area buried in the domain interface is about 797 Å^2 for rhIL-10 versus 2600 Å^2 for IFN-γ.

Superposition of the domains of rhIL-10 and IFN-γ reveals an rms deviation of 1.53 Å for 56 equivalent Cα carbon atoms (Figure 8). The rms deviation drops to 1.15 Å if only residues in helix A and F′ and the AB loop are considered. Although most of the residues in the AB loop are disordered, the positions of the C-terminal end of helix A and the N-terminal end of the AB loop are almost identical in the more restricted alignment. Optimizing the superposition of these segments degrades the alignment of helices B, C, and D. The poorer structural correlation of helices B, C, and D reflects the different interactions of rhIL-10 and IFN-γ at the dimer interface. Specifically, the shorter helices of IFN-γ are stabilized by extensive hydrophobic interactions with helix C of the 2-fold related domain. In contrast, the longer helices of IL-10 are stabilized by a more extensive hydrophobic core and not by interactions at the domain interface.

Analysis of the structural alignment between IL-10 and IFN-γ reveals five residues which are conserved in all amino acid sequences. One additional residue, Lys-138 (rhIL-10 numbering), is conserved in all but one species of IFN-γ. The five conserved residues cluster in the core of the molecules at the pronounced bend (129° in both structures) in helix F (Figure 9). The residues are donated from the AB loop, helix C, and helix F and consist of Leu-47, Phe-71, Tyr-72, Ala-139, and Glu-142 for rhIL-10 and Leu-28, Phe-52, Tyr-53, Ala-109, and Glu-112 for IFN-γ. Phe-71 and Tyr-72 are donated from helix C. The surface created by Phe-71, Tyr-72, and Leu-47 forms a small pocket in which the Cβ of Ala-139 packs. The OH of Tyr-72 forms a hydrogen bond with the carbonyl carbon Ala-139 to satisfy the α-helical hydrogen bonds of helix F. In addition, Oϵ1 and Oϵ2 of Glu-142 form hydrogen bonds with the main-chain nitrogen atoms of Leu-47 and Leu-48 in the AB loop. Analogous interactions are formed in the core of IFN-γ.

DISCUSSION

The crystal structure of IL-10 exhibits the greatest overall structural similarity to IFN-β and IFN-γ which also bind related class 2 cytokine receptors. Although rhIL-10 was known to be a noncovalent dimer in solution, the intercalated dimer resembling the fold of IFN-γ observed in the crystal was not expected. While rhIL-10 is a dimer in the crystal, the observed structural identity between IL-10 and other monomeric cytokines and the limited interaction at the domain interface raise the question: could IL-10 exist as a compact monomer? While no monomeric form of IL-10 has been reported, several examples of monomer−dimer structural rearrangements have been observed (Bennett et al., 1994). To form a stable globular monomer of IL-10 would require helices E and F to fold back into the cleft created by helices A−D of the same chain (e.g., helices E and F superimpose on the positions of helices E′ and F′ in the

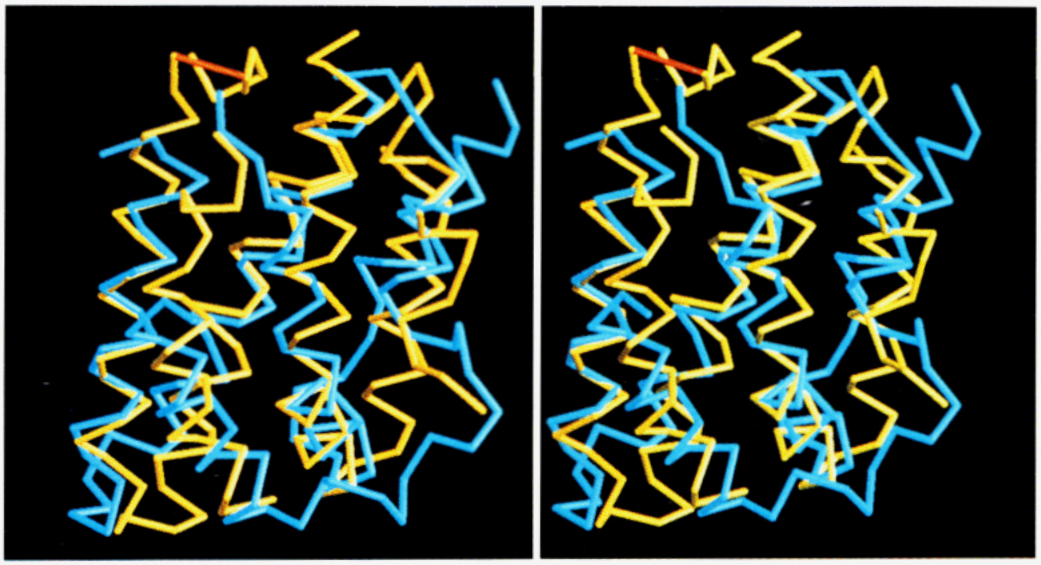

FIGURE 8: Stereoview of the superposition of rhIL-10 (yellow) and IFN-γ (blue) domains. The view is identical to that in Figure 4.

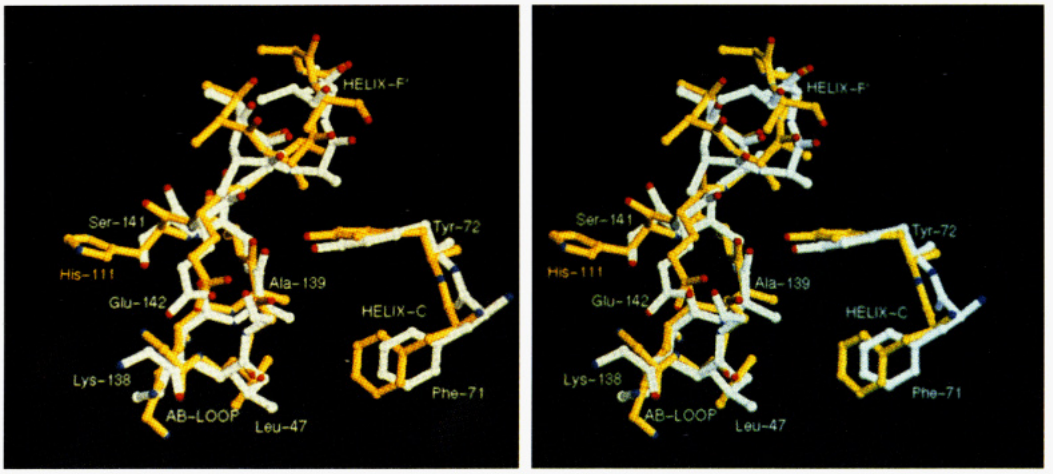

FIGURE 9: Stereoview of the five structurally conserved residues in IL-10 and IFN-γ. The carbon atoms and bonds are colored white for rhIL-10 and yellow for IFN-γ. Nitrogen atoms are colored blue and oxygen atoms red. The conserved residues are labeled according to rhIL-10 numbering (colored white) and consist of Leu-47, Phe-71, Tyr-72, Ala-139, and Glu-142. Lys-138 is conserved in all but one IFN-γ amino acid sequence. Histidine-111 from IFN-γ is labeled in yellow. The importance of His-111 and Ser-141 are discussed in the text.

dimer). Computer modeling experiments to alter the conformations of residues in the DE loop (following Cys-114) to wrap helices E and F into the cleft formed by helices A−D were unsuccessful. The constraint placed on the DE loop by the Cys-62−Cys-114 disulfide bond prohibits the DE loop from adopting a conformation that allows superposition of helices E and F onto helices E′and F′ as observed in the dimer.

Analysis of interactions in the core of IL-10 and IFN-γ reveals a striking structural correspondence of a five-residue cluster at the pronounced bend in helix F (Figures 4 and 9). The conservation of these five residues in all IL-10 and IFN-γ amino acid sequences suggests that they play an important role in stabilizing the 60° bend in helix F as well as the AB loop. It is quite possible that this 5-residue motif (IFN-γ motif) may be used by other cytokines or α-helical proteins to stabilize a similar fold. Conversely, the presence of the motif in other sequences might be used to "fingerprint" other cytokines which exhibit similar core interactions. Analysis of the amino acid sequences of interleukins 3, 6, 7, 9, 11, 12, 13, 14, and 15, which have unknown three-dimensional structures, did not reveal this simple pattern of residues.

Currently, there are no reported mutagenesis or structural studies that define the specific residues that participate in the high-affinity interaction of rhIL-10 with its cell surface receptor. However, on the basis of the structural identity between rhIL-10 and IFN-γ, we have used the large amount of biochemical data on the IFN-γ/IFN-γ receptor interaction (Lundell & Narula, 1994) to construct a potential receptor binding site for IL-10. Peptide mapping (Jarpe & Johnson, 1993) and site-directed mutagenesis (Lunn et al., 1992; Lundell et al., 1994) studies on IFN-γ have identified helix A, the AB loop, and His-111 on helix F′ as important for receptor binding. Remarkably, His-111 is located at the center of the structurally conserved bend in helix F′. On the basis of the structural alignment, the equivalent residue in rhIL-10 (Ser-141) is a likely candidate for interaction with the IL-10 receptor. Analysis of the exposed surface around Ser-141 reveals three hydrophobic residues (Leu-46, Leu-53, and Ile-145) which encircle Tyr-149. These residues might form additional interactions with the IL-10R. The importance of aromatic and hydrophobic residues in forming high-affinity interactions in the growth hormone receptor complex lends supporting evidence to the model (Clackson & Wells, 1995). To further test the putative IL-10R binding site, one domain of IL-10 was superimposed onto the GH structure. Serine-141 and Ile-145 in the IL-10R putative binding site superimpose onto Asp-171 and Thr-175 of GH. Strikingly, these two GH residues have been shown to make direct contact with the growth hormone receptor (de Vos et al., 1992). In contrast to the structural similarity between rhIL-10 and GH around Ser-141 and Ile-145, the AB loops are separated by approximately 19 Å. How much these significant structural differences will alter the IL-10/IL-10 receptor interaction relative to the growth hormone receptor complex model cannot be predicted.

In addition to the conserved structure around helix F′, rhIL-10 and IFN-γ each contain similar flexible regions. Like rhIL-10, the crystal and NMR structures of IFN-γ have shown the AB loop to be highly flexible with no clear secondary structure (Ealick et al., 1991; Samudzi et al., 1991; Grzesiek et al., 1992). This is noteworthy since the AB loop of IFN-γ has been shown to interact with the IFN-γ receptor (Lundell et al., 1994) and the loops are in close proximity with the structurally conserved bend in helix F′. Additional flexible regions which extend away from the core of the molecules are observed at the N-terminus for rhIL-10 and at the C-terminus for IFN-γ. The basic tail of IFN-γ has been identified as important for high-affinity interactions with its receptor (Lundell & Narula, 1994). While no activities have been identified for the N-terminus of IL-10, it is interesting that the IL-10 homolog, BCRF1, which displays significant sequence differences at the N-terminus, also exhibits altered biological function.

NOTE ADDED IN PROOF

After submission of this paper, the crystal structure of recombinant human IL-10, which crystallized in space group $P3_221$, was reported (Zdanov et al., 1995). This structure appears to be similar to ours except that we observe residues 18−37, 45−107, and 111−159 in our electron density maps while residues 12−160 are observed by Zdanov et al. A detailed comparison of the two structures is being initiated.

ACKNOWLEDGMENT

We thank Leigh J. Walter for technical assistance, Keith Wilson and staff at the EMBL for synchrotron time and helpful discussions, Dr. Charles Bugg for coordinates of IFN-γ, Dr. Yukio Mitsui for Cα carbon coordinates of IFN-β, and Anthony Engle and Maxine Rice for help in preparation of the manuscript.

REFERENCES

Abdel-Meguid, S. S., Shieh, H.-S., Smith, W. W., Dayringer, H. E., Violand, B. N., & Bentle, L. A. (1987) *Proc. Natl. Acad. Sci. U.S.A. 84*, 6434−6437.

Aguet, M., Dembic, Z., & Merlin, G. (1988) *Cell 55*, 273−280.

Bazan, J. F. (1990) *Proc. Natl. Acad. Sci. U.S.A. 87*, 6934−6938.

Bennett, M. J., Choe, S., & Eisenberg, D. (1994) *Proc. Natl. Acad. Sci. U.S.A. 91*, 3127−3131.

Blancho, G., Gianello, P., Germana, S., Baetscher, M., Sachs, D. H., & LeGuern, C. (1995) *Proc. Natl. Acad. Sci. U.S.A. 92*, 2800−2804.

Bogdan, C., Vodovotz, Y., & Nathan, C. (1991) *J. Exp. Med. 174*, 1549−1555.

Brooks, B. R., Bruccoleri, R. E., Olafson, B. D., States, D. J., Swaminathan, S., & Karplus, M. (1983) *J. Comput. Chem. 4*, 187−217.

Brünger, A. T. (1989) *Acta Crystallogr. A45*, 42−50.

Brünger, A. (1992a) *X-PLOR Manual, Version 3.1*, Yale University, New Haven, CT.

Brünger, A. (1992b) *Nature 355*, 472−475.

Carson, M. (1991) *J. Appl. Crystallogr. 24*, 958−961.

CCP4 (1994) *Acta Crystallogr. D50*, 760−763.

Chen, W-F., & Zlotnik, A. (1991) *J. Immunol. 147*, 528−534.

Clackson, T., & Wells, J. A. (1995) *Science 267*, 383−386.

Cook, W. J., Windsor, W. T., Murgolo, N. J., Tindall, S. H., Nagabhushan, T. L., & Walter, M. R. (1995) *Proteins: Struct., Funct., Genet. 22*, 187−190.

Cowtan, K. (1994) *J. CCP4 ESF-EACBM Newsl. Protein Crystallogr. 31*, 34−38.

Defrance, T., Vanbervliet, B., Briére, F., Durand, I., Rousset, F., & Banchereau, J. (1992) *J. Exp. Med. 175*, 671−682.

de Vos, A. M., Ultsch, M., & Kossiakoff, A. A. (1992) *Science 255*, 306−312.

de Waal Malefyt, R., Abrams, J., Bennett, B., Figdor, C. G., & de Vries, J. E. (1991a) *J. Exp. Med. 174*, 1209−1220.

de Waal Malefyt, R., Haanen, J., Spits, H., Roncarolo, M-G., te Velde, A., Figdor, C., Johnson, K., Kastelein, R., Yssel, H., & de Vries, J. E. (1991b) *J. Exp. Med. 174*, 915−924.

Ealick, S. E., Cook, W. J., Vijay-Kumar, S., Carson, M., Nagabhushan, T. L., Trotta, P. P., & Bugg, C. E. (1991) *Science 252*, 698−702.

Feng, L., Tang, W. W., Chang, J. C. C., & Wilson, C. B. (1993) *Biochem. Biophys. Res. Commun. 192*, 452−458.

Fiorentino, D. F., Bond, M. W., & Mosmann, T. R. (1989) *J. Exp. Med. 170*, 2081−2095.

Fiorentino, D. F., Zlotnik, A., Mosmann, T. R., Howard, M., & O'Garra, A. (1991) *J. Immunol. 147*, 3815−3822.

Go, N. F., Castle, B. E., Barrett, R., Kastelein, R., Dang, W., Mosmann, T. R., Moore, K. W., & Howard, M. (1990) *J. Exp. Med.*, 1625−1631.

Goodman, R. E., Oblak, J., & Bell, R. G. (1992) *Biochem. Biophys. Res. Commun. 189*, 1−7.

Grzesiek, S., Döbeli, H., Gentz, R., Garotta, G., Labhardt, A. M., & Bax, A. (1992) *Biochemistry 31*, 8180−8190.

Hash, S. M., Brown, W. C., & Rice-Ficht, A. C. (1994) *Gene 139*, 257−261.

Heldin, C. (1995) *Cell 80*, 213−223.

Hill, C. P., Osslund, T. D., & Eisenberg, D. (1993) *Proc. Natl. Acad. Sci. U.S.A. 90*, 5167−5171.

Ho, A. S. Y., Liu, Y., Khan, T. A., Hsu, D.-H., Bazan, J. F., & Moore, K. W. (1993) *Proc. Natl. Acad. Sci. U.S.A. 90*, 11267−11271.

Hsu, D.-H., de Waal Malefyt, R., Fiorentino, D. F., Dang, M.-N., Vieira, P., deVries, J., Spits, H., Mosmann, T. R., & Moore, K. W. (1990) *Science 250*, 830−832.

Jarpe, M. A., & Johnson, H. M. (1993) *J. Interferon Res. 13*, 99−103.

Kabsch, W. (1976) *Acta Crystallogr. A32*, 922−923.

Kabsch, W., & Sander, C. (1983) *Biopolymers 22*, 2577−2637.

Liu, Y., Wei, S. H.-Y., Ho, A. S.-Y., de Waal Malefyt, R., & Moore, K. W. (1994) *J. Immunol. 152*, 1821−1829.

Lovejoy, B., Cascia, D., & Bisenberg, D. (1993) *J. Mol. Biol. 234*, 640−653.

Lundell, D. J., & Narula, S. K. (1994) *Pharmacol. Ther. 64*, 1−21.

Lundell, D., Lunn, C. A., Senior, M. M., Zavodny, P. J., & Narula, S. K. (1994) *J. Biol. Chem. 269*, 16159−16162.

Lunn, C. A., Fossetta, J., Dalgarno, D., Murgolo, N., Windsor, W., Zavodny, P. J., Narula, S. K., & Lundell, D. (1992) *Protein Eng. 5*, 253−257.

MacNeil, I. A., Suda, T., Moore, K. W., Mosmann, T. R., & Zlotnik, A. (1990) *J. Immunol. 145*, 4167−4173.

Milburn, M. V., Hassell, A. M., Lambert, M. H., Jordan, S. R., Proudfoot, A. E. I., Graber, P., & Wells, T. N. C. (1993) *Nature 363*, 172−176.

Moore, K. W., Vieira, P., Fiorentino, D. F., Trounstine, M. L., Khan, T. A., & Mosmann, T. R. (1990) *Science 248*, 1230−1234.

Moore, K. W., Rousset, F., & Banchereau, J. (1991) *Springer Semin. Immunopathol. 13*, 157−166.

Morris, A. L., MacArthur, M. W., Hutchinson, E. G., & Thornton, J. M. (1992) *Proteins 12*, 345−364.

Novick, D., Cohen, B., & Rubinstein, M. (1994) *Cell 77*, 391−400.

Otwinowski, Z. (1993) in *Data Collection and Processing* (Sawyer, L., Isaacs, N., & Bailey, S., Eds.) pp 56−62, SERC Daresbury Laboratory, Warrington.

Rennick, D., Berg, D., & Holland, G. (1992) *Prog. Growth Factor Res. 4*, 207−227.

Rennick, D., Hunte, B., Dang, W., Thompson-Snipes, L., & Hudak, S. (1994) *Exp. Hematol. 22*, 136−141.

Robinson, R. C., Grey, L. M., Staunton, D., Vankelecom, H., Vernalla, A. B., Moreau, J., Stuart, D. I., Heath, J. K., & Jones, E. Y. (1994) *Cell 77*, 1101−1116.

Rode, H.-J., Janssen, W., Rösen-Wolff, A., Bugert, J. J., Thein, P., Becker, Y., & Darai, G. (1993) *Virus Genes 7*, 111−116.

Rousset, F., Garcia, E., Defrance, T., Péronne, C., Vezzio, N., Hsu, D.-H., Kastelein, R., Moore, K. W., & Banchereau (1992) *Proc. Natl. Acad. Sci. U.S.A. 89*, 1890−1893.

Sack, J. S. (1988) *J. Mol. Graphics 6*, 244−245.

Samudzi, C. T., Burton, L. E., & Rubin, J. R. (1991) *J. Biol. Chem. 266*, 21791−21797.

Senda, T., Shimazu, T., Matsuda, S., Kawano, G., Shimizu, H., Nakamura, K. T., & Mitsui, Y. (1992) *EMBO J. 11*, 3193−3201.

Sprang, S. R., & Bazan, J. F. (1993) *Curr. Opin. Struct. Biol. 3*, 815−827.

Suda, T., O'Garra, A., MacNeil, I., Fischer, M., Bond, M. W., & Zlotnik, A. (1990) *Cell. Immunol. 129*, 228−240.

Tan, J. C., Indelicato, S. R., Narula, S. K., Zavodny, P. J., & Chou, C. (1993) *J. Biol. Chem. 268*, 21053−21059.

Thompson-Snipes, L., Dhar, V., Bond, M. W., Mosmann, T. R., Moore, K. W., & Rennick, D. M. (1991) *J. Exp. Med. 173*, 507−510.

Ultsch, M. H., Somers, W., Kossiakoff, A. A., & de Vos, A. M. (1994) *J. Mol. Biol.* 236, 286−299.

Uzé, G., Lutfalla, G., & Gresser, I. (1990) *Cell 60*, 225−234.

Vieira, P., de Waal-Malefyt, R., Dang, M.-N., Johnson, K. E., Kastelein, R., Fiorentino, D. F., deVries, J. E., Roncarolo, M.-G., Mosmann, T. R., & Moore, K. W. (1991) *Proc. Natl. Acad. Sci. U.S.A. 88*, 1172−1176.

Windsor, W. T., Syto, R., Tsarbopoulos, A., Zhang, R., Durkin, J., Baldwin, S., Paliwal, S., Mui, P. W., Pramanik, B., Trotta, P. P., & Tindall, S. H. (1993) *Biochemistry 32*, 8807−8815.

Zdanov, A., Schalk-Hili, Gustchina, A., Tsang, M., Weatherbee, J., & Wlodawer, A. (1995) *Structure 3*, 591−601.

BI951192R